Egyptian Journal of Petroleum (2014) 23, 67–78

Egyptian Petroleum Research Institute

Egyptian Journal of Petroleum

www.elsevier.com/locate/egyjp
www.sciencedirect.com

FULL LENGTH ARTICLE

Mineralogical, geochemical and hydrocarbon potential of subsurface Cretaceous shales, Northern Western Desert, Egypt

D.A. Mousa [a], A.A. Abdou [a], N.H. El Gendy [b], M.G. Shehata [a], M.A. Kassab [a], A.A. Abuhagaza [a,*]

[a] Egyptian Petroleum Research Institute, EPRI, Cairo, Egypt
[b] Geology Department, Faculty of Science, Tanta University, Egypt

Received 2 July 2013; accepted 23 October 2013
Available online 22 April 2014

KEYWORDS

Mineralogy;
Geochemistry;
Hydrocarbon potentiality;
Subsurface;
Shale;
North Western Desert

Abstract Twenty four Cretaceous shale core samples of Gibb Afia-1, Betty-1, Salam-1X and Mersa Matruh-1 wells were mineralogically and geochemically studied using XRD, XRF and Rock Eval Pyrolysis. Kaolinite, smectite and illite are the main clay minerals in addition to rare chlorite, while the non-clay minerals include quartz, calcite, dolomite and rare siderite. The shales were derived through intensive chemical weathering of mafic basement and older sedimentary rocks. These sediments were deposited in a near-shore shallow marine environment with some terrestrial material input. The shales have poor to fair organic content. It is marginally to rarely mature.

1. Introduction

Cretaceous sediments cover a wide area of the surface of Egypt [1]. The subsurface of the Northern Western Desert comprises a number of structurally controlled sedimentary basins where several rock facies were deposited [2]. Exploration activities in the Northern Western Desert led to significant oil and gas discoveries in the Cretaceous rocks [3]. The hydrocarbon potentiality of the Lower Cretaceous source rocks in the North Western Desert basin have been discussed by many authors; [4] mentioned that the Lower Cretaceous (Alam El Bueib Fm.) is an effective source rock for hydrocarbon accumulation in the south Matruh area. [5] stated that the Lower Cretaceous might act as an important source for oil generation in Bade El Din Concession. [6] recognized that the oils from Alam El Bueib and Bahariya reservoirs are genetically related, multisourced from Khatatba and Alam El Bueib source rocks with minor contribution from Kohla source rocks. [7] showed that the Khatatba Formation entered the early stage of hydrocarbon generation during Late Cretaceous–Eocene. Alam El Bueib Formation during Late Cretaceous–Oligocene. Bahariya Formation is still immature and does not reach the onset of hydrocarbon generation. It is interesting to get more information about the shale facies as one of the most important oil and gas source rocks. For this reason; the shale core samples from four wells namely Gibb Afia-1, Betty-1, Salam-1X and Mersa

* Corresponding author.
E-mail address: aaa_geo107@yahoo.com (A.A. Abuhagaza).
Peer review under responsibility of Egyptian Petroleum Research Institute.

Production and hosting by Elsevier

1110-0621 © 2014 Production and hosting by Elsevier B.V. on behalf of Egyptian Petroleum Research Institute.
Open access under CC BY-NC-ND license. http://dx.doi.org/10.1016/j.ejpe.2014.02.010

Matruh-1 (Fig. 1) were mineralogically and geochemically studied to define their characteristics, condition of deposition and hydrocarbon potentiality.

2. Sampling and methodology

Twenty five shale samples were selected from the four wells for the present study. Distribution of these samples is illustrated in (Fig. 2). Thirteen samples were analyzed by XRD by using the oriented method to define their clay minerals, and four samples of them were analyzed by the bulk method.

About 20 g of each sample for the oriented method is granulated, treated with HCl (3%) to dissolve carbonate, H_2O_2 and carefully washed several times with distilled water, then sieved using 0.063 mm sieve, shacked and dispersed in one-liter cylinder. Three oriented slides were prepared for each sample by sedimentation of clay fraction drawn off at a depth of 10 cm. from the suspension surface on clean glass slides after 24 h [8,9]. The first slide was used as untreated specimen, the second was saturated with ethylene glycol and the third was heated at 550 °C for two hours and slowly cooled. The analyses were carried out at the laboratories of Egyptian Petroleum Research Institute (EPRI) using a Phillips apparatus model X' Pert PRO, PANalytical, Netherland. Twenty two samples were geochemically analyzed by XRF for their major and trace elements. The analyses were carried out at the Egyptian Applied Research Laboratories, CMRDI using a Phillips PW 1404 WD-XRF via program "POWDER". Fourteen samples were analyzed using Rock Eval 6 analyzer at the laboratories of EPRI to study their organic contents and hydrocarbon potential.

3. Stratigraphy

The Cretaceous rocks in the studied area are divided into Lower Cretaceous and Upper Cretaceous units [10] as shown in (Fig. 3). The following is a brief description of these units from top to bottom:

3.1. Khoman formation (Santonian–Maestrichtian)

It consists mainly of fractured chalk, filled with calcite crystals. Ali et al. [11] reported that, the lower part of the Khoman Formation is composed of shales and carbonate interbeds. The chalk unconformably overlies the Abu Roash Formation or Bahariya Formation and unconformably underlies the Lower Eocene to Oligocene rock units.

3.2. Abu roash formation (Late Cenomanian – Santonian)

It conformably overlies the Bahariya Formation and unconformably underlies the Khoman Formation. The formation is divided into seven informal members designated from bottom to top: G, F, E, D, C, B and A. Members B, D and F are relatively pure carbonate, whereas A, C, E and G members are largely fine clastics. The Abu Roash Formation was deposited in an open shallow marine shelf during several sedimentary cycles [12].

3.3. Bahariya formation (Early Cenomanian)

It consists of glauconitic and pyritic sandstone interbedded with shales, siltstones and carbonates [13]. It conformably overlies the Kharita Formation and underlies the Abu Roash Formation. Bahariya Formation was deposited under fluvio-marine environment in the Western Desert [13].

3.4. Kharita formation (Early Cretaceous – Albian)

It consists of sandstone and a few shale interbeds of shallow marine origin that extends over most of the Western Desert [3]. It conformably overlies the Dahab Formation and

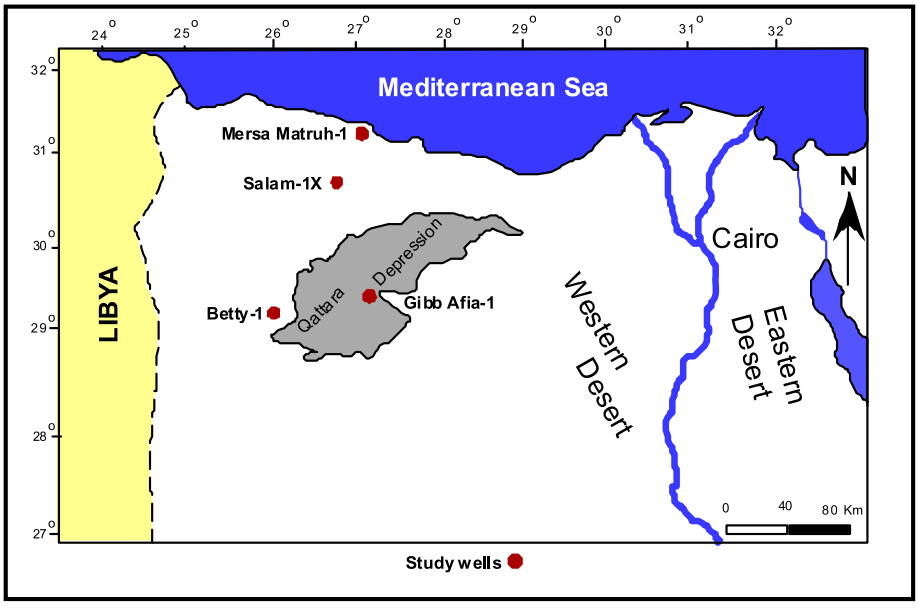

Figure 1 Location map of the studied wells.

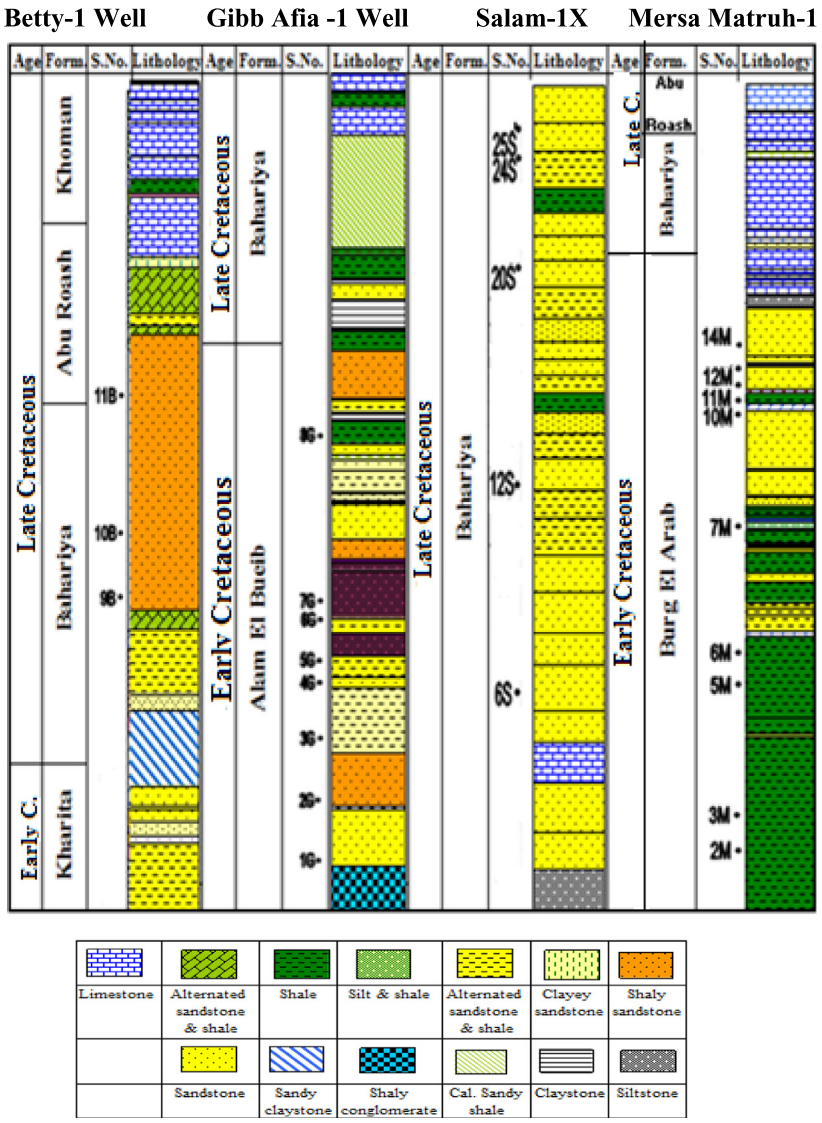

Figure 2 Distribution of the studied shale samples.

underlies the Bahariya Formation. The Kharita Formation is considered as a very good reservoir [13,14]. It is also considered as a fair to good source rock in the Matruh basin [15].

3.5. Dahab formation (Aptian – Early Albian)

It consists of shales, siltstones, sandstones and minor carbonate interbeds that conformably overlies the Alamein Formation and conformably underlies the Kharita Formation. The shales of the Dahab Formation were believed to be the most effective vertical and possibly the lateral seal for the underlying Alamein Dolomite reservoir [16]. The sandstones of Dahab Formation are considered as the producing interval in the Alamein and the Razzak fields [17].

3.6. Alamein formation (Early Cretaceous – Middle Aptian)

It corresponds to the carbonate unit (composed of light brown, microcrystalline dolomite and a few thin shale interbeds) which conformably overlies the Burg El Arab Formation and conformably underlies the Dahab Formation. It is deposited under subtidal shallow marine conditions of moderate energy [13]. The Alamein Formation consists mainly of dolomite and limestone of shallow marine origin [13].

3.7. Burg El Arab formation

According to oil companies [18]; it is a sequence of fine to coarse clastics that either conformably overlies the Masajid Formation or unconformably overlies the Wadi Natrun, the Bahrein, the Paleozoic rock units or the basement rocks. The Burg El-Arab Formation conformably underlies the Bahariya Formation. It was divided into four members: Alam El Buieb, Kharita, Alamein Dolomite and Dahab Shale members.

3.8. Alam El Bueib formation (Neocomian – Early Aptian)

It consists of sandstone that interbedded with minor shale layers of shallow marine or fluvio-deltaic environments [13].

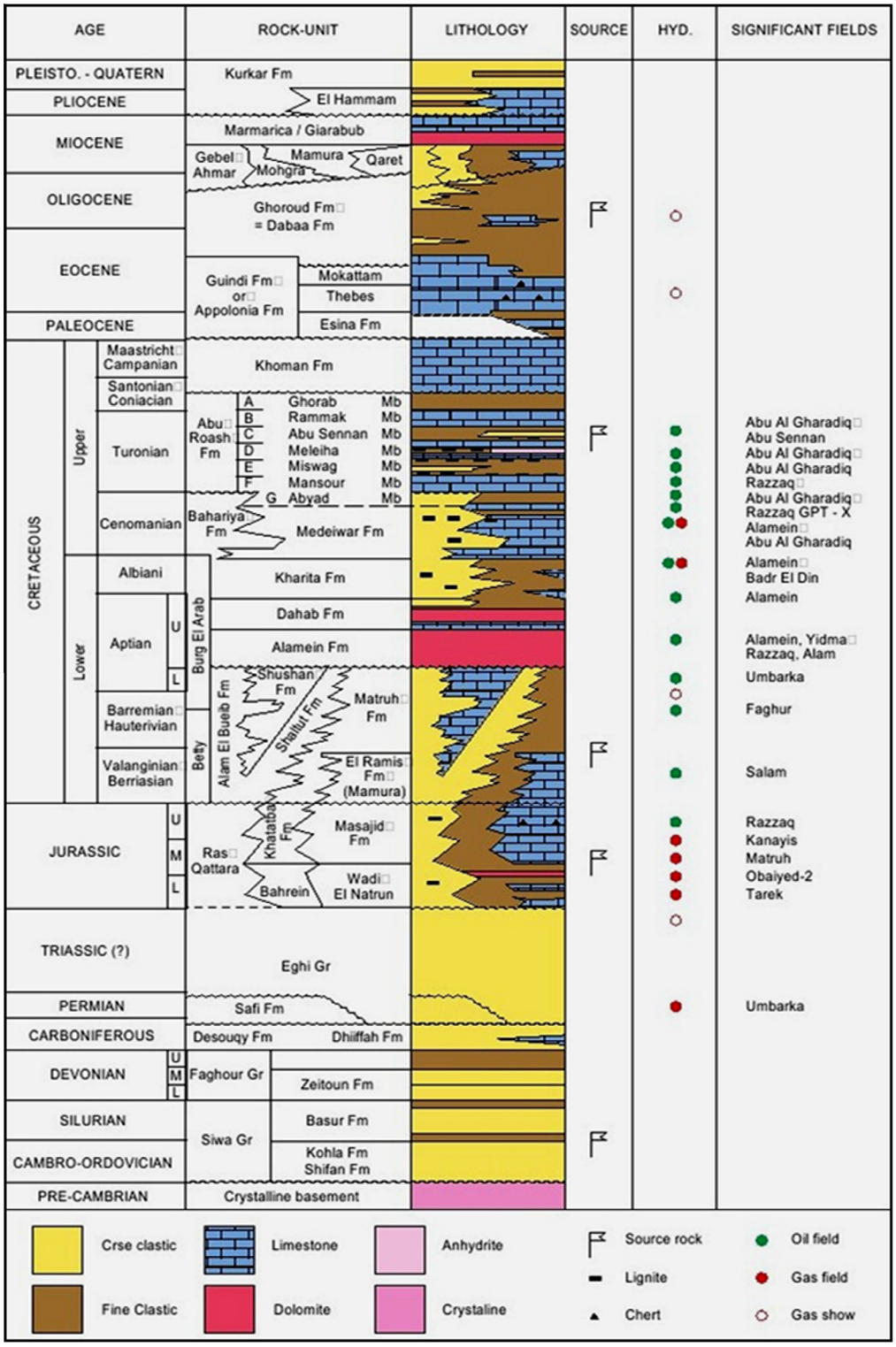

Figure 3 Lithostratigraphic Column of the northern part of the Western Desert [10,19].

4. Mineralogical composition

The mineralogical composition of both oriented and bulk samples was studied by the X-ray diffraction analysis. Semiquantitative estimations of minerals were carried out using the peak height [20]. The identification of these minerals was carried out using the A.S.T.M cards according to [21]. The main constituent minerals and their frequencies are given in (Tables 1 and 2).

Table 1 The relative proportions of the mineralogical constituents of the studied bulk samples.

Age	Form.	Well name	S. No.	Mineralogical composition %		
				Quartz	Siderite	Clay
Late cretaceous	Bahariya	Salam-1X	20S	93.5		6.51
			12S	80.3	12.45	7.25
		Betty-1	11B	95.3		4.7
Early cretaceous	Burg El Arab	Mersa Matruh-1	6M	55.12	36.64	8.24

Table 2 Semi-quantitative clay mineral percentage of the studied samples.

Age	Formation	Well name	S. No.	Clay minerals		
				Kaolinite	Illite	Smectite
Late cretaceous	Bahariya	Salam-1X	25S	97.2	–	2.8
			24S	98.2	1.8	–
			20S	96.5	–	3.5
			12S	97.1	–	2.9
			6S	95.6	–	4.4
		Betty-1	11B	83.5	–	16.5
Early cretaceous	Alam El Bueib	Gibb Afia-1	6G	96.3	3.7	–
			5G	96.7	3.34	–
	Burg El Arab	Mersa Matruh-1	7M	94.9	–	5.1
			6M	86.4	13.6	–
			5M	95.9	–	4.1
			3M	97.1	–	2.9
			2M	92.9	7.1	–

5. Non-clay minerals

5.1. Quartz

Quartz is identified with its reflections at 4.27, 3.34 and 2.45 Å (Fig. 4) in varying frequencies all over the studied Cretaceous succession with an average of 26.7% and 77.13% for the Lower and Upper Cretaceous samples respectively. The amount of quartz may be indicative of shoreline proximity [22]. Quartz may be either detrital [22], diagenetic [23] or biogenic [24].

5.2. Siderite

Siderite is recorded at d-spacings 2.79, 2.13 and 1.73 Å (Fig. 4). It is commonly formed as concretions in marine shales [22] and indicates intermediate Eh values.

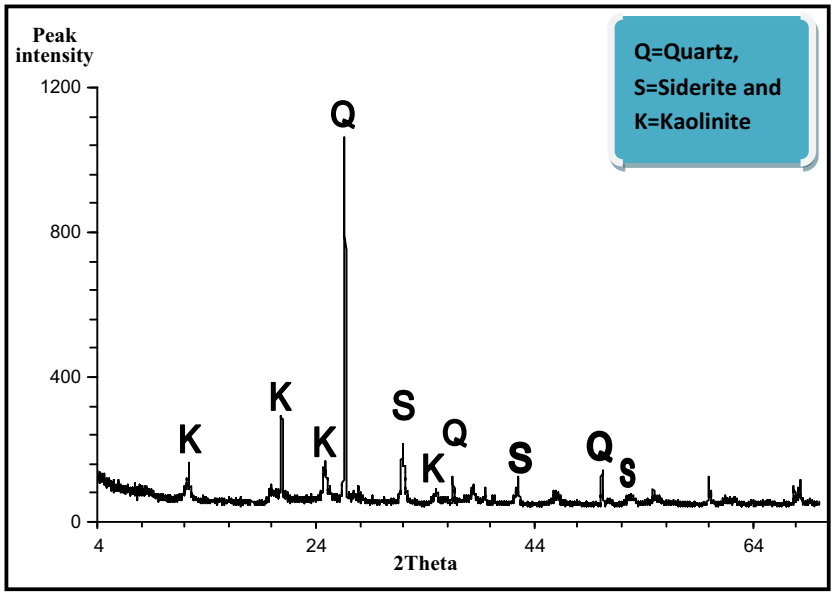

Figure 4 X-ray diffraction chart of a representative bulk sample (12S) from Salam-1X well.

6. Clay minerals

6.1. Kaolinite

Kaolinite is the most abundant clay mineral in the investigated samples (Fig. 5), it is characterized by d-spacings at 7.16–7.29 and 3.58–3.6 Å. The basal reflection is characterized by sharp peaks, which may reflect the high order of crystallinity of the mineral in most samples [25,26]. The semiquantative estimation of kaolinite content in the studied samples is 94.8% and 95.02% for the Lower and Upper Cretaceous rocks respectively.

Kaolinite is generally formed in warm moist regions as a residual weathering product, or sometimes by hydrothermal alteration of other aluminosilicate minerals especially feldspars [27]. The high content of kaolinite suggests a high degree of weathering in the tropical continental environments [28]. In marine basins; kaolinite is concentrated in the near shore area [22].

6.2. Smectite

Smectite is recorded in a few samples of the studied Lower and Upper Cretaceous rocks following kaolinite in abundance,

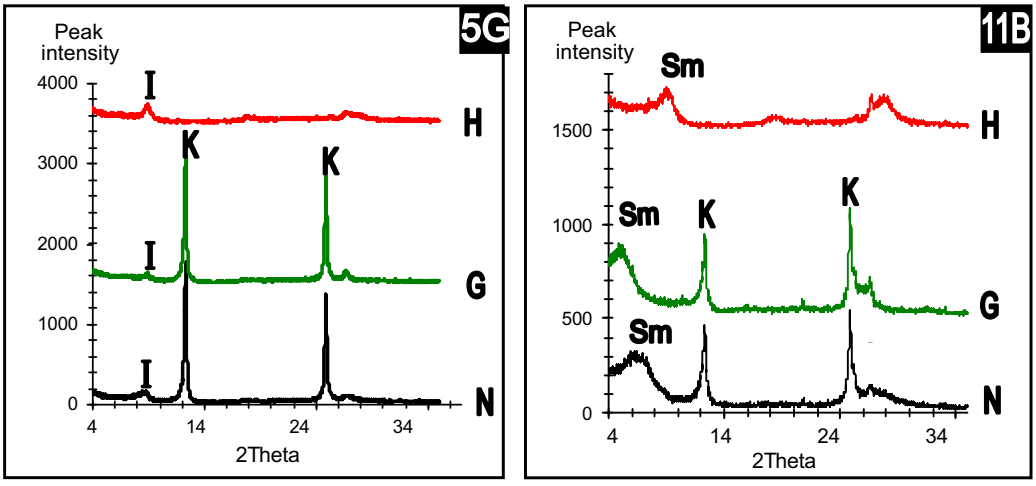

Figure 5 X-ray diffraction patterns of oriented clay fractions from Betty-1 and Gibb Afia-1 wells.

Table 3 Major and trace element frequencies of the studied shale samples.

S. No.	Age	Form.	SiO_2 (%)	Al_2O_3 (%)	TiO_2 (%)	Fe_2O_3 (%)	MgO (%)	CaO (%)	Na_2O (%)	K_2O (%)	P_2O_3 (%)	Sr (ppm)	Co (ppm)	Cr (ppm)	Ni (ppm)
11-B	Late	Bahariya	62.69	19.49	1.76	5.18	1.39	0.44	1.47	1.48	0.18	1522	259.5	68.42	463.6
10-B	Cretaceous		64.92	20.36	2.34	3.62	1.27	0.46	1.18	2.13	0.16	1488	353.9	65.00	675.8
9-B			66.88	19.52	2.06	3.16	1.23	0.41	1.11	2.06	0.16	1522	322.5	65.00	620.8
9-G			61.11	17.31	1.24	7.69	1.72	0.31	0.99	3.09	0.17	1522	188.8	51.32	518.6
25-S			51.2	16.95	1.99	9.96	3.10	1.98	2.03	1.86	0.35	2114	235.9	68.42	510.8
24-S			52.61	16.46	2.14	9.14	3.07	1.92	2.02	1.85	0.32	1860	228	68.42	471.5
23-S			51.85	16.52	2.19	9.16	3.08	1.95	2.03	1.87	0.36	2283	243.8	68.42	487
20-S			55.99	20.01	0.87	7.32	2.49	0.24	1.05	4.95	0.27	143.8	322.5	58.16	628.6
12-S			51.8	18.13	1.11	10.14	1.99	2.05	1.53	1.82	0.90	1606.6	298.9	68.42	432
6-S			64.05	23.45	1.54	2.94	0.89	0.22	1.26	1.42	0.18	1352.9	267.4	68.42	487
8-G	Early	Alam El	54.55	21.27	1.30	8.87	1.24	0.98	1.51	0.97	0.35	1581	243.8	68.42	785.8
7-G	Cretaceous	Bueib	55.81	20.16	1.46	7.48	1.37	0.79	1.23	2.24	0.29	1513.6	298.9	78.69	715.1
5-G			54.19	20.56	1.67	7.83	1.49	0.82	1.11	2.43	0.34	1479.8	361.8	71.85	887.9
4-G			56.6	20.48	1.3	6.99	1.5	0.57	1.09	2.66	0.32	1462.9	338.2	65.00	848.6
2-G			58	21.09	1.41	7.5	1.21	0.23	0.18	1.71	0.38	1522	298.9	68.42	589.3
1-G			52.99	29.08	1.77	3.0	0.76	0.26	0.72	1.26	0.36	1471	361.8	85.53	919.4
14-M		Burg El	47.28	21.12	1.12	8.0	1.74	5.98	1.22	1.34	0.21	1496.7	173	58.16	746.5
12-M		Arab	56.67	22.97	1.12	5.2	1.01	0.41	1.50	0.96	0.19	1513.6	289.9	71.85	447.9
11-M			55.4	22.79	1.52	6.8	1.21	0.52	1.62	1.37	0.23	1522	291	65.00	581.5
10-M			56.6	21.76	1.50	6.2	1.22	0.48	1.64	1.41	0.22	1488	212	68.42	510.8
7-M			56.62	21.64	1.28	6.7	1.34	0.49	1.14	2.33	0.24	1471	416.8	61.58	612.9
5-M			56.51	15.73	1.69	7.5	1.94	1.17	3.34	1.34	0.30	1606.6	283	68.42	628.6
3-M			54.95	18.50	1.32	8.3	1.88	0.94	1.35	1.27	0.23	1606.6	306.7	68.42	722.9
1-M			54.58	19.13	1.84	7.3	1.94	1.03	1.70	1.71	0.25	1691	353.9	68.42	612.9

especially those of the Upper Cretaceous samples (Fig. 5). The pattern of the air dried specimens revealed broad basal reflections ranging from 12.2 to 14.9 Å. These reflections expand on glycolation to a range of 16–18 A° and collapse to 10 Å on heating to 550 °C due to the loss of interlayer water [29–31]. Roser and Korsch [32] stated that the 12 Å smectite corresponds to a Na-smectite with one H_2O molecule while a 14 Å smectite is a Ca-variety. The important source of smectite is the weathering of ferromagnesian minerals [33] and the alteration of volcanic glass; it is favored by alkaline condition and converts to illite during burial diagenesis [34].

6.3. Illite

It is recorded in a few of the studied samples especially those of the Early Cretaceous, it is identified at d-spacings 10.20, 10.19, 10.04, 9.34 and 5.01 Å which are neither affected by glycolation nor heating. The semiquantitative estimation of illite in the studied samples is 8.6% and 1.8% for the Lower and Upper Cretaceous sediments respectively. Illite is often produced from the weathering of feldspars, micas and pre-existing shales as well as the transformation of smectite in deeply buried muds and shales, it is often found in temperate environments under neutral or slightly alkaline conditions [33].

7. Inorganic geochemistry

Geochemical signatures of clastic sedimentary rocks provide important sources of information that record different aspects of provenance and environments of deposition [32]. The frequencies of the chemical components of the studied shale

Table 4 Pearson's correlation coefficient values of each pair of elements of the studied samples.

	SiO_2	Al_2O_3	TiO_2	Fe_2O_3	MgO	CaO	Na_2O	K_2O	P_2O_3	Sr	Co	Cr	Ni
SiO_2	1.00												
Al_2O_3	0.0	1.00											
TiO_2	0.22	−0.20	1.00										
Fe_2O_3	−0.70	−0.64	−0.23	1.00									
MgO	−0.48	−0.76	0.22	0.71	1.00								
CaO	−0.65	−0.25	−0.07	0.46	0.41	1.00							
Na_2O	−0.23	−0.56	0.28	0.34	0.49	0.23	1.00						
K_2O	0.13	−0.22	−0.21	0.1	0.31	−0.21	−0.27	1.00					
P_2O_3	−0.46	−0.16	−0.23	0.55	0.27	0.20	0.07	−0.03	1.00				
Sr	−0.24	−0.33	0.55	0.30	0.29	0.29	0.38	−0.63	0.15	1.00			
Co	0.21	0.34	0.13	−0.37	−0.32	−0.41	−0.27	0.21	0.01	−0.26	1.00		
Cr	−0.12	0.35	0.40	−0.24	−0.22	−0.20	0.002	−0.31	0.03	0.18	0.40	1.00	
Ni	−0.18	0.42	−0.06	−0.14	−0.33	0.02	−0.32	0.07	−0.09	−0.21	0.40	0.24	1.00

Table 5 Geochemical parameters and functions of the studied shale.

S. No.	Age	Form.	F1	F2	CIW	PIA	CIA	SiO2/Al2O3	Ni/Co ppm	WIP	V	STI
11-B	Late Cretaceous	Bahariya	0.68	−3.13	91.07	90.41	85.18	3.22	1.79	2241.3	6.4	71.37
10-B			−1.77	−1.77	92.55	91.75	84.38	3.19	1.91	2585.1	7.7	70
9-B			−2.05	−2.01	92.78	91.99	84.50	3.43	1.92	2477.5	7.9	71.56
9-G			−0.61	−2.99	93.01	91.62	79.78	3.53	2.75	3271.5	6.8	73.81
25-S			0.56	−4.3	80.87	79.01	74.28	3.02	2.17	3275.3	2.7	69.04
24-S			−0.6	−1.12	80.69	78.76	73.98	3.20	2.07	3249.7	2.6	69.31
23-S			−0.66	−4.03	80.59	78.64	73.85	3.14	2.00	3276.8	2.6	68.91
20-S			−2.04	−1.02	93.94	92.11	76.23	2.80	1.95	4871	6.6	71.38
12-S			4.47	−4.16	83.51	82.00	77.05	2.86	1.45	2844.3	3.6	70.86
6-S			2.37	−2.29	94.06	93.70	88.99	2.73	1.82	1984.1	11	69.84
8-G	Early Cretaceous	Alam El Bueib	6.5	−4.37	89.52	89.07	86.01	2.56	3.22	1916.6	6	68.92
7-G			2.56	−2.88	90.89	89.87	82.56	2.77	2.39	2759.9	6.6	69.75
5-G			2.24	−2.87	91.42	90.38	82.50	2.64	2.45	2861	6.7	68.46
4-G			1.74	−2.66	92.50	91.48	82.58	2.76	2.51	2999	7.3	70.16
2-G			3.51	−4.26	98.09	97.93	90.87	2.75	1.97	1638.2	14	69.91
1-G			5.57	−2.69	96.74	96.60	92.85	1.82	2.54	1541	17	62.13
14-M		Burg El Arab	7.84	−2.5	74.58	73.31	71.21	2.24	4.32	2816.8	2.5	66.68
12-M			5.14	−3.45	92.32	92.02	88.89	2.47	1.50	1795.9	8.2	68.77
11-M			4.84	−3.09	91.42	90.92	86.65	2.43	2.00	2230.4	7.2	67.66
10-M			3.76	−2.98	91.12	90.57	86.04	2.60	2.41	2269.3	6.9	68.8
7-M			2.85	−2.76	93.00	92.22	84.53	2.62	1.47	2734.3	8.1	69.38
5-M			1.05	−1.76	77.72	76.14	72.89	3.59	2.22	3363.3	2.7	72.16
3-M			2.97	−4.98	88.99	88.27	83.86	2.97	2.36	2130.6	4.7	71.02
1-M			1.29	−3.34	87.51	86.45	81.16	2.85	1.73	2702.1	4.5	69.12

samples are given in (Table 3). Comparison of these data with the published average shales (Table 4) illustrates that the studied shales are within the range of silica and sodium; with higher contents of aluminum, titanium and iron while their contents of Mg, Ca and K are lower than the published data. The higher Al content may indicate fineness in grain size and presence of kaolinite; the higher Fe content may indicate the occurrence of pyrite, siderite or iron silicates while the lower content of Mg and K may indicate marine and lagoonal conditions [35].

8. Provenance

Several major and trace element-based discrimination diagrams have been proposed to infer the source/provenance of siliciclastic rocks [32,36–39].

Discrimination functions (F1 and F2) were calculated (Table 5) following the equations of [32] since:

$$\text{Discriminant function(F1)} = (-1.773 \times TiO_2\%) + (0.607 \times Al_2O_3\%) + (0.76 \times Fe_2O_3\%) + (-1.5 \times MgO\%) + (0.616 \times CaO\%) + (0.509 \times Na_2O\%) + (-1.22 \times K_2O\%) + (-9.09).$$

$$\text{Discriminant function(F2)} = (0.445 \times TiO_2\%) + (0.07 \times Al_2O_3\%) + (-0.25 \times Fe_2O_3\%) + (-1.142 \times MgO\%) + (0.432 \times Na_2O\%) + (1.426 \times K_2O\%) + (-6.861).$$

These functions were plotted (Fig. 6A) on the discrimination diagram of [32] where the Lower Cretaceous samples fall within the field of mafic and intermediate igneous rocks while

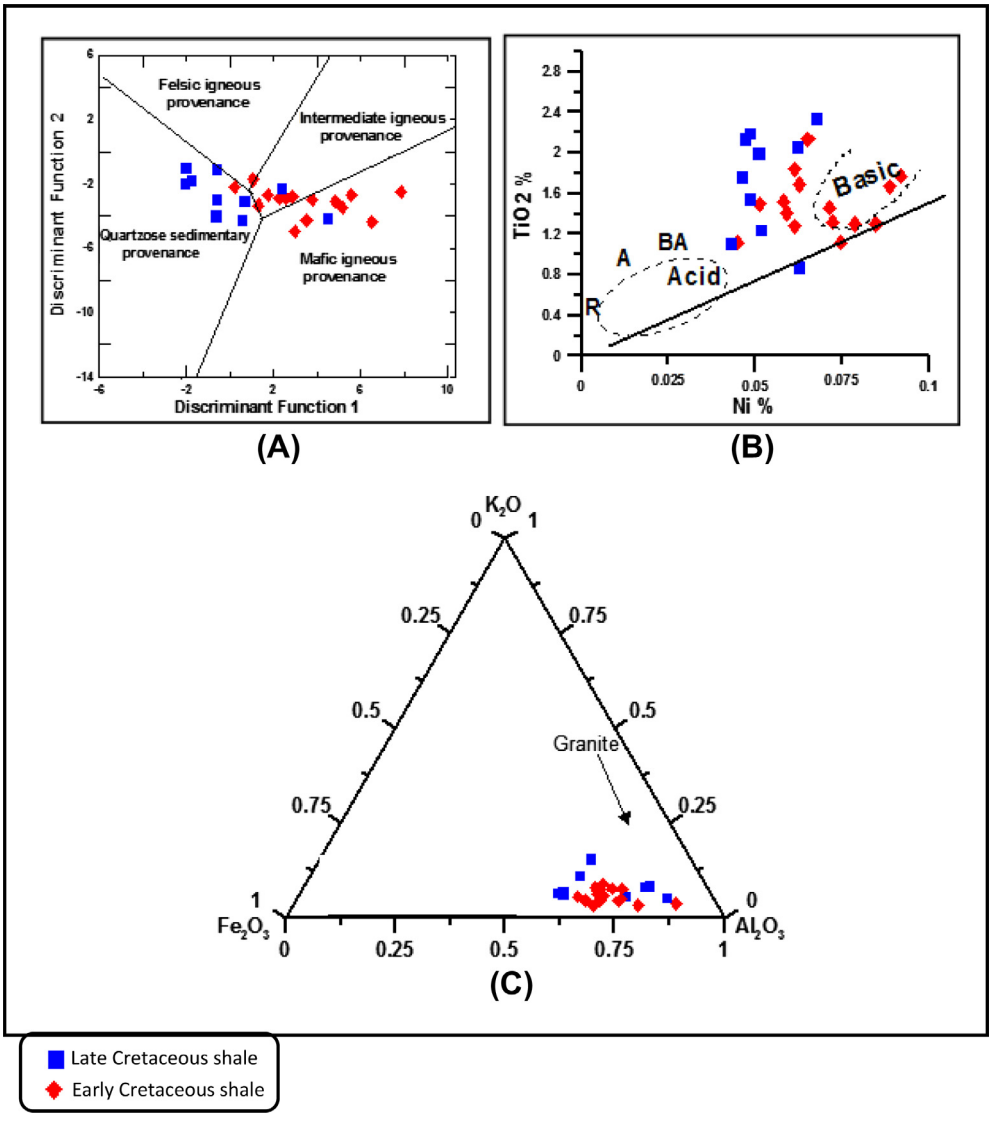

Figure 6 Provenance discrimination diagrams for the studied shales: (A) after [32], (B) [39] and (C) after [37].

the Upper Cretaceous samples fall within the field of quartzose sedimentary provenance. On the TiO_2 wt.% vs. Ni% diagram (Fig. 6B) established by [39]; the shales of the studied Lower and Upper Cretaceous samples lie in the basic and around the basic field. On the Fe_2O_3–K_2O–Al_2O_3 ternary diagram (Fig. 6C) established by [37]; the studied Lower and the Upper Cretaceous shale samples plot away from the granite field.

9. Weathering

Chemical weathering indices (CIA), sometimes referred to as indices of alteration, are commonly used for characterizing and evaluating weathering profiles [34]. Chemical weathering indices incorporate bulk major element oxide chemistry into a single value for each sample. Application of different indices (Table 5) indicates high values which mean intensive chemical weathering in the source area [30,40–43].

Much of the chemical variation resulting from weathering may be expressed in the system Al_2O_3–[CaO–Na_2O]–K_2O shown by the ternary diagram of [44] (Fig. 7A), where unweathered rocks are clustered along the left hand side of the K-feldspar-plagioclase join [44]. All the studied samples plot towing the Al_2O_3-[CaO–Na_2O] edge and Al_2O_3 apex. This reflects the preponderance of aluminous clay minerals within the studied samples and the depletion in K. CIA of the studied samples increased from 66.5 (CIA values of feldspar and biotite = 50) to 94.5 (CIA values of illite = 80 and kaolinite = 100). Obviously the highest degree of alteration (in terms of CIA) is compatible with the sediments having maximum kaolinite and less feldspar content. The CIA values increase upward with the increase in kaolinite and decrease in feldspar content.

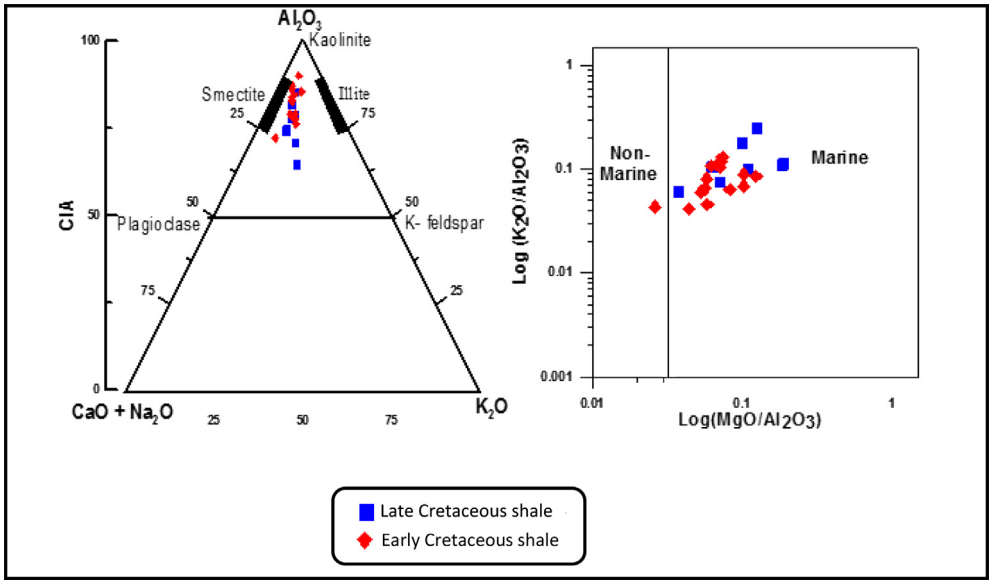

Figure 7 (A) Plotting of the chemical analysis data of the studied shales on Al_2O_3–[CaO–Na_2O]–K_2O ternary diagram of [28] and (B) depositional environment diagram on log (MgO/Al_2O_3) and log (K_2O/Al_2O_3) of [45].

Table 6 Pyrolysis data for the lower and upper cretaceous samples.

Well name	Fm.	Age	S. No.	TOC wt. %	S_2 mg/g	T_{ma} °C	HI, mg HC/g TOC	OI, mg CO_2/g TOC
Betty-1	Bahariya	Late Cretaceous	11B	0.68	0.25	430	37	96
Salam -1			25S	1.33	0.99	439	74	73
			24S	0.89	0.83	434	93	25
			20S	0.41	0.58	433	141	0
			12S	0.73	0.49	435	67	41
			6S	0.96	0.72	435	75	29
Gibb Afia-1	Alam El -Buieb	Early Cretaceous	6G	0.08	0.09	321	113	275
			5G	0.31	0.57	431	184	81
Mersa Matruh -1	Burg El Arab		10M	0.73	0.98	437	134	5
			7M	1.37	0.61	433	45	47
			6M	0.32	0.21	438	66	72
			5M	0.24	0.31	434	129	13
			3M	1.19	0.45	453	38	27
			2M	1.1	0.32	469	29	30

10. Depositional environment

The relation between MgO/Al_2O_3 and K_2O/Al_2O_3 was used by [45] to differentiate between marine and non-marine clay. Application of this relation on the studied Lower and Upper Cretaceous shales (Fig. 7B) revealed that all the studied samples fell within the marine environment. According to [46]; values of Ni/Co ratio below 5 indicate oxic environment whereas values above 5 suggest suboxic and anoxic environment. Ni/Co ratio of the studied Lower Cretaceous shale samples ranges from 1.47 to 3.22 (average = 2.32) and the same ratio for the studied Upper Cretaceous shale samples varies from 1.45 to 2.75 (average = 1.98). These low values of Ni/Co ratio suggest deposition under oxic conditions [46]. In conclusion, the studied shales were deposited in a shallow marine environment under oxic conditions.

11. Rock–eval pyrolysis

The rock Eval pyrolysis analyses were carried out for fourteen shale samples collected from the four studied wells. The resultant data (Table 6) were used to provide information about organic richness type of organic matter and thermal maturation of the shale samples.

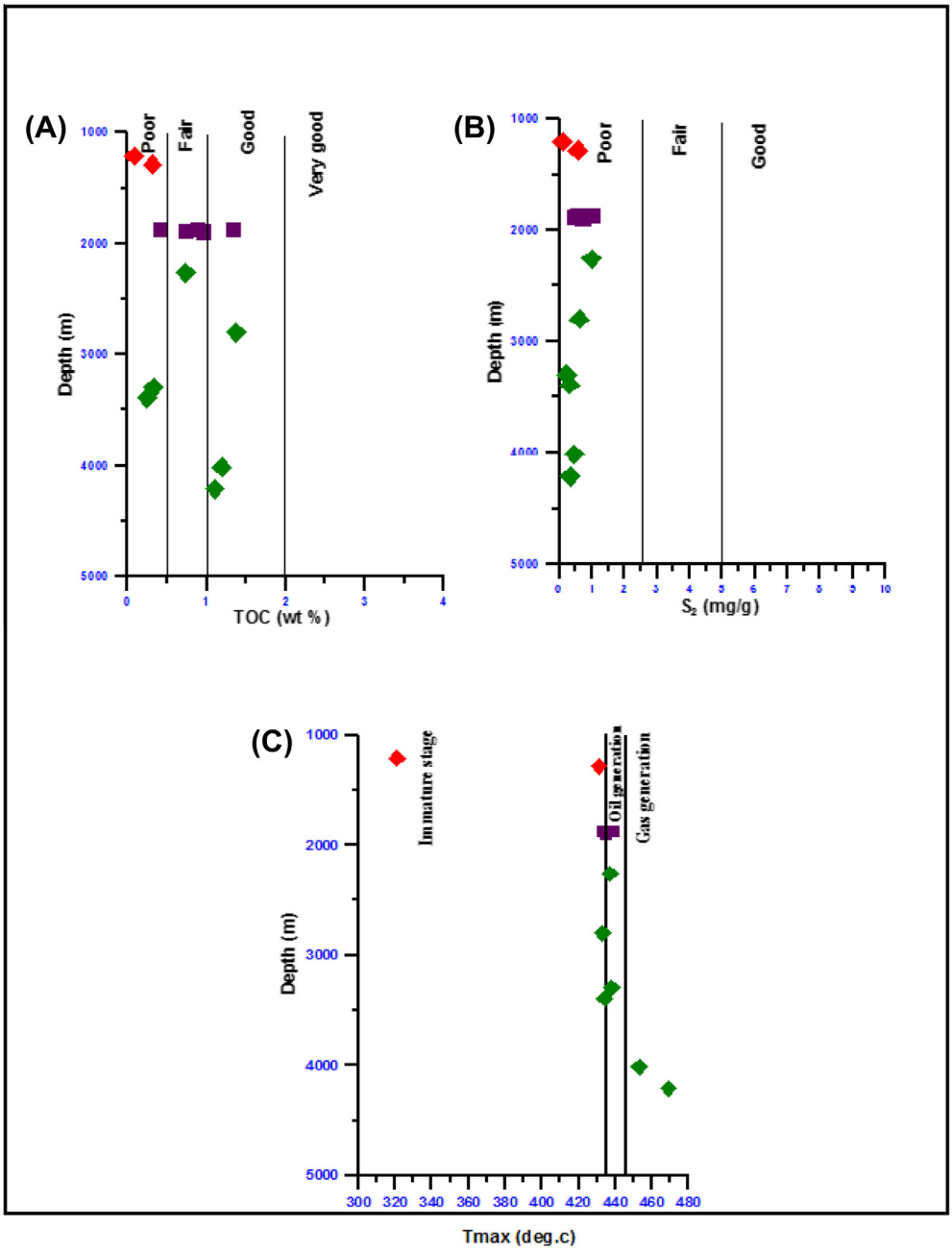

Figure 8 Source rock parameters of the studied samples. (A) Organic richness (TOC wt.%), (B) oil potentiality S_2 (mg/g), and (C) thermal maturity by T_{max}.

11. Organic richness

The organic richness represented by the total organic carbon (TOC) of the Lower Cretaceous shale samples represented by Burg El Arab and Alam El Bueib formations ranges from 0.08 to 1.37 wt.% (Table 6). The studied samples lie in the poor to good zone (Fig. 8A). In the Upper Cretaceous shale samples represented by Bahariya Formation, the total organic carbon ranges from 0.41 to 1.33 wt.% that represents poor to good organic richness of the studied samples (Fig. 8A) [47].

12. Hydrocarbon potentiality

The hydrocarbon potentiality (S_2) values for the Lower Cretaceous shale samples range from 0.09 to 0.9 (Table 6, Fig. 8B) which show that the shale samples lie in the poor zone. The hydrocarbon potentiality of the Upper Cretaceous shale samples also indicate a poor zone (Fig. 8B), with S_2 values ranging from 0.25 to 0.99.

13. Thermal maturation

The T_{max} value is the temperature at the maximum point of "S_2" peak released from Rock-Eval Pyrolysis. It is used to determine the degree of maturity of the sedimentary organic matter. The T_{max} value for the studied Lower Cretaceous shale samples shows mainly oil generation (Fig. 8C) as the T_{max} values range from 321 to 469 °C (Table 6). A few shale samples lie in the immature and gas generation stages (Fig. 8C) [47]. The Upper Cretaceous shale samples show oil generation (Fig. 8C), as the T_{max} values range from 430 to 439 °C (Table 6).

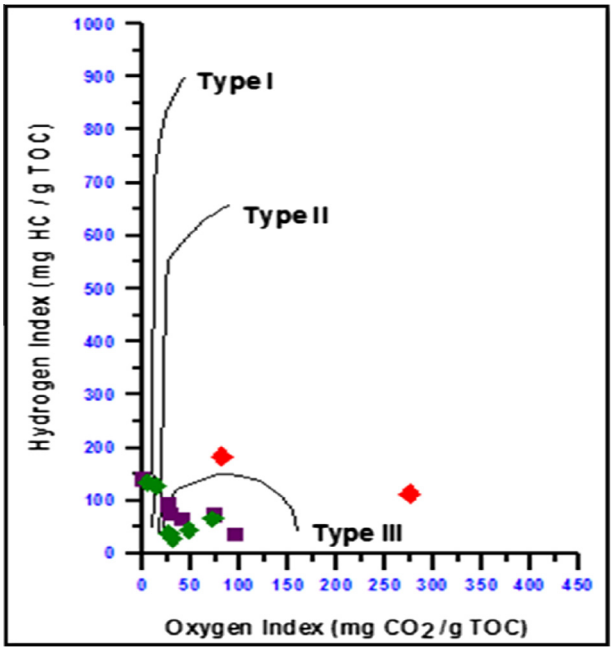

Figure 9 Modified Van Krevelen type diagram showing kerogen type of the studied samples after [48].

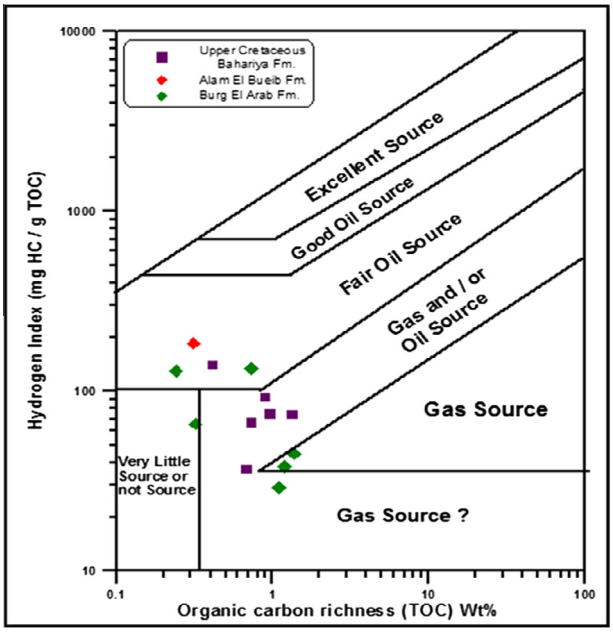

Figure 10 Source rock characterization using plot of HI vs. TOC for Upper and Lower Cretaceous samples after [49].

14. Genetic type of organic matter

The Lower Cretaceous shale samples contain type III/II kerogen as shown in (Fig. 9), as the hydrogen index (HI) values range from 29 to 184 mg/g TOC (Table 6) indicating the capability of these formations to generate mixed gas and oil, [48] (Fig. 10). The Upper Cretaceous Bahariya Formation samples contain mainly type III kerogen as shown in (Fig. 9) with HI values ranging from 37 to 141 mg/g TOC (Table 6) indicating the capability of producing mainly gas and/or oil source (Fig. 10) as the organic input is mainly terrestrial organic matter.

15. Conclusions

The mineralogical composition of the studied Cretaceous shales is predominated by kaolinite and quartz in addition to a variable ratio of smectite, siderite and illite. These shales are characterized by a low Mg and K as well as high Al and Fe contents. They were formed through intensive weathering of intermediate and mafic igneous rocks and reworking of older sediments of the Late Cretaceous. Mineralogical and geochemical studies (organic and inorganic) indicate deposition of these shales under a shallow marine environment with some terrestrial input. The studied shales have poor to good organic richness mainly type III/II kerogen indicating terrestrial input. They indicate the capability to produce gas and fair oil source.

References

[1] R. Said, (Ed.), The Geology of Egypt, A.A. Balkema, Rotterdam, Book field, published for the EGPC, CONOCO Hurghada Inc., and REPSOL Exploration, S.A., 1990 (pp. 1–734).

[2] B. Issawi, M. El Hinnawi, M. Francis, A. Mazhar, Egypt. Geol. Surv. (1999) 76.
[3] J.R. Parker, Hydrocarbon habitat of the Western Desert, Egypt: 6th EGPC Exploration and Production Conference, vol. 1, 1982 (p. 106).
[4] L.M. Sharaf, M.F. Ghanem, S.A. Hussein, M.M. El Nady, J. Sedim. Egypt 7 (1999) 71–81.
[5] M.M. El Nady, M.M. Hammad, J. Environ. Sci. 20 (2000) 25–51.
[6] L.M. Sharaf, M.M. El Nady, J. Egypt. Sedimentol. 11 (2003) 61–76.
[7] M.M. El Nady, F.M. Ghanem, Egypt. Energy Source 33 (23) (2011) 2218–2229.
[8] German Muller, Sedimentary Petrology, Part 1, Methods in Sedimentary Petrology (Hans-Ulrich Schmincke, Trans.), Hafner Publishing Co., 1967 (p. 383).
[9] J.E. Gillot, Clay in Engineering Geology, El-Sevier, 1968.
[10] Schlumberger, Well evaluation conference of Egypt, Technical Editing Services, Chester, 1995, p. 87.
[11] S.A. Ali, G. Besher, G. Ammar, Razzak oil field stratigraphic study, GUPCO internal report, unpublished, 1989, p. 16.
[12] S.H. Wasfi, Cahiers Micropal. 3 (1973) 89–121.
[13] EGPC (Egyptian General Petroleum Corporation, Western Desert, oil and gas fields, a comprehensive overview. EGPC 11th Petrol. Explor. And Prod. Confer. Cairo, 1992 (pp. 1–431).
[14] EGPC (Egyptian General Petroleum Corporation), History of oil exploration, Egypt. EGPC 8th Petrol. Explor. And Prod. Confer. Cairo, 1986 (pp. 1–34).
[15] M.F. Ghanem, M. Hammad, A.F. Maky, Organo source analyses of the subsurface Lower Cretaceous rocks in the vicinity of Matruh basin, North Western Desert, Egypt. 4th Inter. Confer. Geology of the Arab world Cairo Univ., 1998 (p. 104).
[16] A.S. Abdine, S. Deibis, Lower Cretaceous–Aptian sediments and their oil prospects in the Northern Western Desert, Egypt. 8th Arab Petrol. Cogr. Algiers, vol. 74 (B-3), 1972 (p. 17).
[17] O.A. El Shaarawy, A. Abdel Aal, P. Papazis, H. Helmy, North Western Desert 349–2 (IF 36–4) well. Recommendation, GUPCO internal report, unpublished, 1989, pp. 1–22.
[18] G. Hanter, North Western Desert, in: R. Said (Ed.), The Geology of Egypt, Balkema, 1990, pp. 293–319.
[19] Schlumberger, Well evaluation conference of Egypt. Schlumberger Middle East Service, 1984, p. 64.
[20] J. Thorez. In: G. Lelotte, Dison, Belgique (Eds.), Practical Identification of Clay Minerals: A Handbook for Teachers and Students in Clay Mineralogy, Belgique, 1976, p. 90.
[21] G.E. Brown, The X-ray identification and crystal structure of clay mineral, Mineralogical Society, London, 1961, p. 544.
[22] E.P. Potter, B. Maynard, A.W. Pryor, Sedimentology of Shale, Springer, New York, 1980, pp. 310–270.
[23] Scheiber et al, in: E.P. Potter, B. Maynard, A.W. Pryor (Eds.), Sedimentology of Shale, Springer, New York, 2000, pp. 270–310.
[24] Marta et al, in: E.P. Potter, B. Maynard, A.W. Pryor (Eds.), Sedimentology of Shale, Springer, New York, 1977, pp. 270–310.
[25] L.G. Schultz, Quantitative Interpretation of Mineralogical Composition from X-ray and Chemical Data for the Pierre Shale Geol. Surrv. Profess. Paper, 391-C, U.S. Gov. printing office, Washington, USA, 1964
[26] R.F. Girm, Clay Mineralogy, second ed., McGraw-Hill, New York, 1968, p. 59.
[27] D.M. Moore, R.C. Reynolds, X-ray Diffraction and Identification and Analysis of Clay Mineral, Oxford University Press, New York, 1989, p. 332.
[28] R.J. Gibbs, Geol. Soc. Am. Bull. 78 (1967) 1203–1232.
[29] G. Millot, Geology of Clays, Springer-Verlag, Heidelberg, 1970, p. 429.
[30] G.E. Brown, The X-ray Identification and Crystal Structures of Clay Minerals, Clay Minerals Group, London, 1972, p. 544.
[31] D.R. Prothero, F. Schwab, An Introduction to Sedimentary Rocks and Stratigraphy, W.H. Freeman and Company, New York, 1996.
[32] B.P. Roser, R.J. Korsch, Chem. Geol. 67 (1988) 119–139.
[33] U.S. de Jayawardena, E. Izawa, Eng. Geol. 36 (1994) 303–310.
[34] J.R. Price, M.A. Velbel, J. Chem. Geol. 202 (2003) 397–416.
[35] F.J. Pettijohn, Sedimentary Rocks, third ed., Harper & Row, New York, 1975, p. 628.
[36] P.A. Floyd, W. Franke, R. Shail, W. Dorr, Geol. Rundsch. 69 (1990) 611–626.
[37] K.C. Condie, Chem. Geol. 104 (1993) 1–37.
[38] S.M. McLennan, S. Hemming, D.K. Mcdaniel, G.N. Hanson, Geochemical approaches to sedimentation, provenance and tectonics. In: J.M. Johnsson, A. Basu (Eds.), Processes Controlling the Composition of Clastic Sediments, Geol. Soc. Am., Spec., 1993, pp. 21–40 (Paper 284).
[39] P.A. Floyd, W. Franke, R. Shail, W. Dorr, Precam. Res. 45 (1989) 203–214.
[40] A. Parker, Geol. Mag. 107 (1970) 501–504.
[41] T. Vogt, Norges GeologiskeUndersokelse 121 (1927) 1–560 (in Norwegian, with Englishabstract).
[42] L. Harnois, Sed. Geol. 55 (1988) 319–322.
[43] C.M. Fedo, H.W. Nesbitt, G.M. Young, Geology 23 (1995) 921–924.
[44] H.W. Nesbitt, G.M. Young, Nature 299 (1982) 715–717.
[45] E. Roaldest, Mineralogical and chemical changes during weathering, transportation and sedimentation in different environments with particular references to the distribution of Yttrium and lanthanide elements (Ph.D. thesis), Geol. Inst., Univ. of Oslo, Norway, 1978
[46] B. Jones, D.C. Manning, Chem. Geol. 111 (1994) 111–129.
[47] K.E. Peters, AAPG Bull. 70 (1986) 318–329.
[48] J. Espitalié, J.L. La Porte, J. Madec, F. Marquis, P. Le Plat, J. Paulet, A. Boutefeu, Rev. Inst. Fr. Pet. 32 (1977) 23–42.
[49] K.S. Jackson, P.J. Hawkins, A.J.R. Bennett, APEA J. 20 (1985) 143–158.